Available online at www.sciencedirect.com

SciVerse ScienceDirect

Ceramics International 39 (2013) 2989–2994

CERAMICS INTERNATIONAL

www.elsevier.com/locate/ceramint

One-step room-temperature solid-phase synthesis of $ZnFe_2O_4$ nanomaterials and its excellent gas-sensing property

Yali Cao[a], Dianzeng Jia[a,*], Pengfei Hu[b], Ruiying Wang[a]

[a]*Key Laboratory of Advanced Functional Materials of Autonomous Region, Key Laboratory of Clean Energy Material and Technology of Ministry of Education, Institute of Applied Chemistry, Xinjiang University, Urumqi, Xinjiang 830046, China*
[b]*Laboratory for Microstructures, Shanghai University, Shanghai 200444, China*

Received 10 September 2012; received in revised form 22 September 2012; accepted 23 September 2012
Available online 28 September 2012

Abstract

$ZnFe_2O_4$ nanomaterials have been synthesized by simple one-step solid-phase chemical reaction between $Zn(CH_3COO)_2 \cdot 2H_2O$, $FeCl_3 \cdot 9H_2O$ and NaOH within a very short time at room temperature. The solid-phase products were characterized by X-ray diffraction, energy-dispersive X-ray spectroscopy, thermogravimetic analysis, transmission electron microscopy and scanning electron microscopy. Results indicated that the particle size of product can be obviously let up and the agglomeration phenomenon can be improved by the surfactant. Moreover, the $ZnFe_2O_4$ nanomaterials were applied in gas sensor and exhibited much better sensing performance than bulk $ZnFe_2O_4$. The as-prepared $ZnFe_2O_4$ nanomaterials have high sensitivity, good selectivity and fast response/recovery characteristic for ethanol and hydrogen sulfide. The improved $ZnFe_2O_4$ nanomaterials have high response value of 21.5 and 14.8 for ethanol and hydrogen sulfide in the optimized operating temperature of 332 °C and 240 °C, respectively. The response and recovery time was found to be within 4 s and 14 s for ethanol, while 7 s and 25 s for hydrogen sulfide.
© 2012 Elsevier Ltd and Techna Group S.r.l. All rights reserved.

Keywords: E. Sensors; Nanomaterials; Oxides; Solid-phase synthesis

1. Introduction

Semiconducting binary metal oxides (SBMOs) nanomaterials have attracted considerable attention in recent years for their application to the development of nanoscale electronic and optoelectronic devices [1,2]. As sensing materials of gas sensor, some SBMOs such as ZnO, Fe_2O_3, SnO_2, WO_3 have been extensively investigated and exhibited high sensitivity to target gases in adequate operating temperature [3–6]. However, the selectivity for different gases is still out of control. In recent years, the ternary metal composite oxides (TMCOs) have been developed to attain the better selectivity [7–11]. Most research for TMCOs was focused on thin films [12–14], and there are a few reports on TMCOs nanomaterials in past years [15–18].

TMCOs nanomaterials have been fabricated by hydrothermal synthesis, sol–gel method, coprecipitation method, high-temperature solid-phase method and so on [10,19–24]. High-temperature solid-phase synthesis has become an important method for TMCOs nanomaterials because of its advantage of simple process and high yield. However, high temperature above 900 °C and long time is usually required, which result in the high energy-consumption and long time-consuming. Low-heating solid-phase synthesis that was applied at low temperature less than 100 °C has been studied and developed to synthesize some inorganic nanomaterials in recent years [25–30]. This method has attracted more and more attention due to the simple process, low energy-consumption and mild condition.

In this paper, a simple and effective approach to the solid-phase chemical synthesis of $ZnFe_2O_4$ nanomaterials is demonstrated, which is low-cost and proceeds at room temperature. Especially, the synthesis route that avoids multi-step process used by other methods requires only a simple grinding process and finished within a very short

*Corresponding author. Tel./fax: +86 991 8588883.
E-mail address: jdz0991@gmail.com (D. Jia).

0272-8842/$ - see front matter © 2012 Elsevier Ltd and Techna Group S.r.l. All rights reserved.
http://dx.doi.org/10.1016/j.ceramint.2012.09.076

time. The method may provide a path to fabricate ferrite spinel (AB_2O_4) materials with a convenient and economical way. Furthermore, the gas-sensing characteristics of as-prepared $ZnFe_2O_4$ nanoparticles were performed to explore its possible applications.

2. Experimental

2.1. Synthesis

All the reagents were analytically pure from commercial sources and used without further purification. Typical synthesis for $ZnFe_2O_4$ nanoparticles was as follows. 10 mmol of solid $Zn(CH_3COO)_2 \cdot 2H_2O$ and $FeCl_3 \cdot 9H_2O$ were apart weighed and ground for about 5 min in an agate mortar, then mixed and blended 6 mL polyethylene glycol 600 (PEG 600). After the mixture was ground for 5 min, it was allowed to stand for 5 min. The mixture was mixed with 60 mmol of solid NaOH power and ground. The reaction immediately started when contacting each other. The mixture was continually ground for another 5 min, and the by-product salt, PEG 600 and excess NaOH were washed away with distilled water and alcohol in ultrasonic bath and dried in air to obtain the final product powders and named as sample A. Another experiment without the adding of PEG 600 has been carried out simultaneously and the final product powders were named as sample B. The reaction process can be described as follows:

$$Zn(CH_3COO)_2 + NaOH \rightarrow ZnO + H_2O + CH_3COONa \quad (1)$$

$$FeCl_3 + NaOH \rightarrow Fe_2O_3 + H_2O + NaCl \quad (2)$$

$$ZnO + Fe_2O_3 \rightarrow ZnFe_2O_4 \quad (3)$$

2.2. Characterization

Power X-ray diffraction (XRD) patterns were recorded on a MAC Science MXP18AHF X-ray diffractometer equipped with graphite-monochromatized CuKα radiation ($\lambda = 1.54056$ Å). Energy disperse X-ray spectrum (EDS) was examined on Oxford 2000 energy disperse X-ray spectroscopy. The thermogravimetric analysis (TGA) of the product was examined in air on a NETZSCH STA449C thermal analyzer. Transmission electron microscopic (TEM) images and SAED patterns were obtained on a Hitachi H-600 transmission electron microscopy. Scanning electron microscopy (SEM) image was performed on a LEO1430VP scanning electron microscopy.

2.3. Fabrication of gas sensor

To fabricate thick film sensors, an appropriate quantity of terpineol was added to the $ZnFe_2O_4$ nanoparticles, and the mixture was ground in an agate mortar to form paste. The alumina ceramic tube, which was assembled with platinum wire electrodes for electrical contacts, was dipped into the paste for several times to form gas sensing film. Then the elements were dried in air and annealed at 300 °C for 1 h to evaporate the terpineol. Finally, the alumina tube obtained with a Ni–Cr heater fixed inside was welded onto a bakelite substrate. To improve the stability and repeatability, the sensors were aged at 300 °C for 7 days in air prior to use.

2.4. Measurement of gas sensing properties

Gas sensing characteristics of $ZnFe_2O_4$ nanoparticles were measured in a glass test chamber using the gas-sensing measuring system of HW-30A (Hanwei Electronics Co. Ltd., PR China) under laboratory conditions (28 °C, 34% relative humidity). The working temperature of sensors was adjusted by changing the voltage across the heater side. By monitoring the output voltage across the sensor, the resistances of the sensor in air or in test gas can be measured. The gas response (response magnitude) of the sensors was determined as the R_{air}/R_{gas} ratio, where R_{air} is the resistance of the thick film sensors in air, and R_{gas} is that in the mixture of testing gases and air. The response time is defined as the time required for the conductance to reach 90% of the equilibrium value after the test gas is injected. The recovery time is the time necessary for the sensor to attain a conductance 10% above the original value in air.

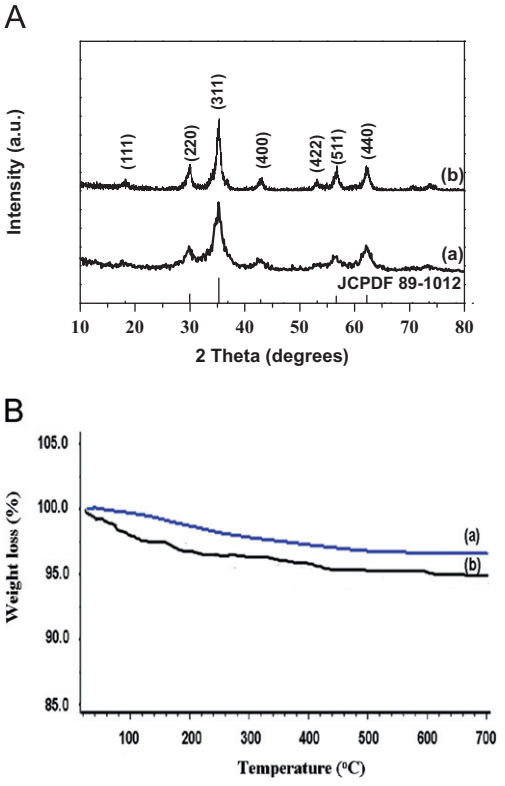

Fig. 1. (A) XRD patterns of (a) sample A and (b) sample B; (B) TG curves of (a) sample A and (b) sample B.

3. Results and discussion

3.1. Structure characterization

Fig. 1(A) shows the XRD patterns of products prepared by one-step room-temperature solid-phase chemical reaction. The samples A and B have broad diffraction peaks that are quite similar to each other, which indicated the small particle size. Compared to standard patterns of $ZnFe_2O_4$ (JCPDF Card file No.89-1012), the maximum position of each broad peak is consisting of that of main peak. The lattice constants obtained by refinement of XRD data for the as-synthesized $ZnFe_2O_4$ are $a=8.433$ Å, $b=8.432$ Å and $c=8.434$ Å, which were consisting of those of standard cubic phase $ZnFe_2O_4$. No characteristic peaks of impurities, such as reactants and other by-product were observed in the samples. The EDS result of the sample revealed the presence of Zn, Fe and O with atomic ratio of 1.02: 2: 4.19. From Fig. 1(B), a weight loss about 4% was observed for the samples A and B attributing to the dehydration of physically adsorbed water. These results indicate that $ZnFe_2O_4$ have been prepared by one-step process of room-temperature solid-phase chemical reaction between two corresponding metal salts and NaOH, which avoids the further process as the annealing process in the solution synthesis or high-temperature solid-phase synthesis.

3.2. Morphology characterization

Fig. 2(a–d) shows the morphology of the samples A and B prepared by one-step solid-phase chemical reaction. From the SEM images with the same magnification, it can be seen that the dominant components of two samples are nano-particles, and the serious agglomeration phenomenon exists

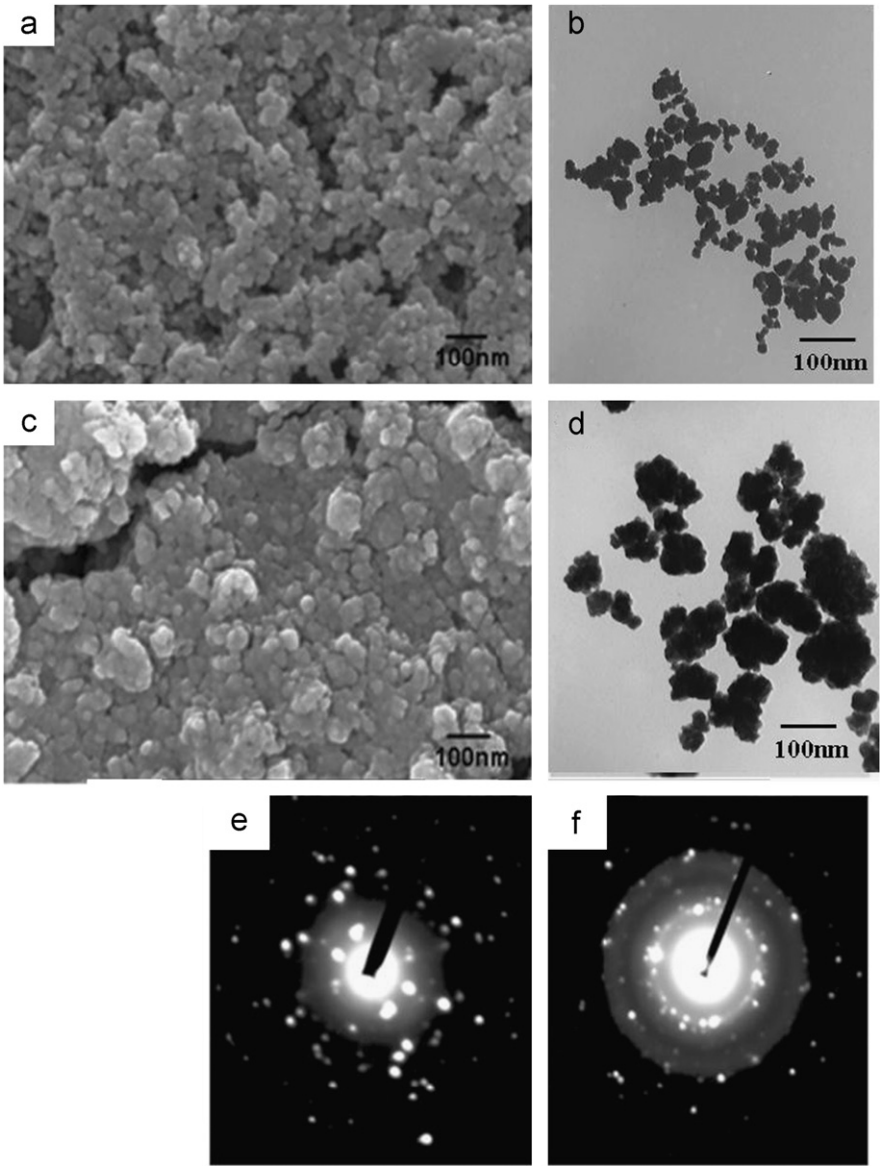

Fig. 2. SEM and TEM images of (a and b) sample A and (c and d) sample B respectively; SAED patterns of (e) sample A and (f) sample B.

in sample B, which frequently occurred for the fabrication of nanomaterials. The sample A with a uniform size distribution has smaller size than sample B. The typical TEM images of samples A and B indicated the same results. A corresponding SAED pattern of samples shown in Fig. 2(e) and (f) suggests that the products have good crystallinity, which can also be supported by their high intensity (>2000) in XRD patterns.

In this study, the $ZnFe_2O_4$ nanomaterials were obtained by one-step solid-phase chemical reaction. The particle size of solid-phase reaction product can be obviously let up through the added surfactant. Simultaneously, the agglomeration phenomenon can be also improved. It was caused from the change of the solid-phase reaction microenvironments. Here, PEG 600 was introduced into the solid-phase reaction system and got involved in the reaction process. In such solid-phase reaction microenvironments, the product particles are encapsulated in the closed or half-closed shells of the surfactant molecules, which blocks up the continued growth and agglomeration of the product particles. Thus the added surfactant, PEG 600 changes the reaction microenvironments, which influences the growth process of solid-phase chemical reaction resulting in the smaller size and better dispersity of the final product. We have attempted to introduce other surfactants into this reaction system, the similar results were obtained. Based on that, the conclusion can be reached that the surfactant can serve as useful medium of solid-phase chemical reaction for the improvement of particle morphology.

3.3. Gas sensing characterization

Nine kinds of gases were selected as a detecting gas to characterize the gas sensing properties of $ZnFe_2O_4$ nanoparticles prepared by one-step solid-phase chemical reaction. Fig. 3 shows the relationship between working temperature and response of sensor to various gases including ethanol (C_2H_5OH), hydrogen sulfide (H_2S), methanal (HCHO), 93# gasoline, xylene ($C_6H_4(CH_3)_2$), ethoxyethane ($(CH_3CH_2)_2O$), liquefied petroleum gas (LPG), hydrogen (H_2) and ammonia (NH_3). The sensitivity change curves of nine gases indicate that the sensors based on $ZnFe_2O_4$ nanoparticles have good response properties. The sensor has high signal response for ethanol and H_2S. The response value of sensor based on sample A can reach to 21.5 and 14.8 at the working temperature about 332 °C, and that based on sample B is 14.2 and 11.3 for 100 ppm ethanol and H_2S at the working temperature about 240 °C, which is higher than bulk $ZnFe_2O_4$ and some reported results of SnO_2/Fe_2O_3 multilayer thin film and ferrite spinel nanomaterials [31,32].

The sample A has higher sensitivity than sample B, which results from the different size and state of aggregation of sample. Changes in size and state of aggregation of $ZnFe_2O_4$ can result in the variations in gas-sensing properties of synthesized materials because they have different surface-to-volume ratios and the surface defects which may be the active core to adsorb the testing gas. The tiny and disperse nanoparticles may be a favorable factor for the response signal caused by the chemical interaction between testing gases and the $ZnFe_2O_4$ surface.

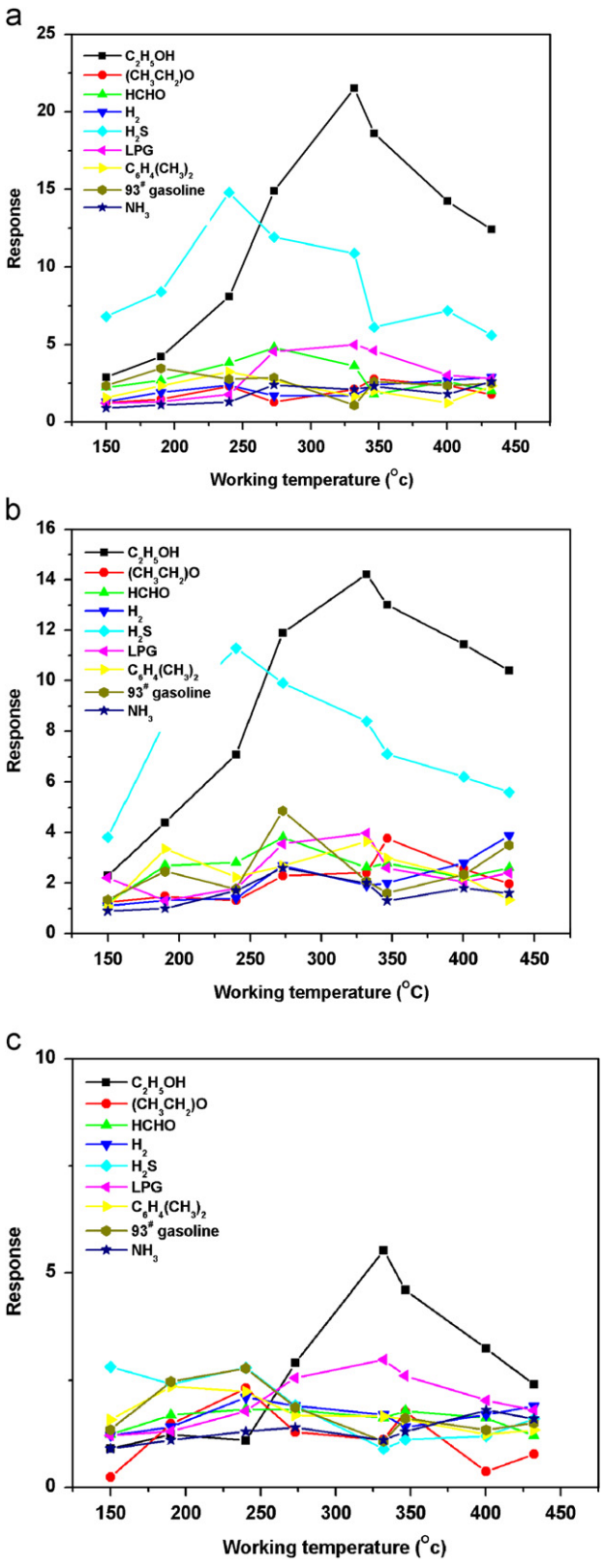

Fig. 3. Relationship between working temperature and response of sensor to various gases (100 ppm) of (a) sample A, (b) sample B and (c) bulk $ZnFe_2O_4$.

The variation in sensitivity with ethanol and hydrogen sulfide concentration is shown in Fig. 4. It can be observed that the sensor response increased with an increase of ethanol and hydrogen sulfide gas concentration. They began responding at 20 ppm low concentration, and did not reach the saturation until the 500 ppm high concentration, which indicated wide-concentration response characteristics for ethanol and hydrogen sulfide.

Fig. 5 shows the response/recovery characteristics of $ZnFe_2O_4$. The response time and the recovery time of sample A to 100 ppm ethanol are 4 s and 14 s, and that to 100 ppm hydrogen sulfide were about 7 s and 25 s, which is shorter than that for sample B of 8 s and 15 s for ethanol and 13 s and 28 s for hydrogen sulfide. The response/recovery time of two $ZnFe_2O_4$ nanomaterials is far shorter than bulk $ZnFe_2O_4$ that is 25 s for the response time and 70 s for the recovery time. This may be because the nanomaterials have

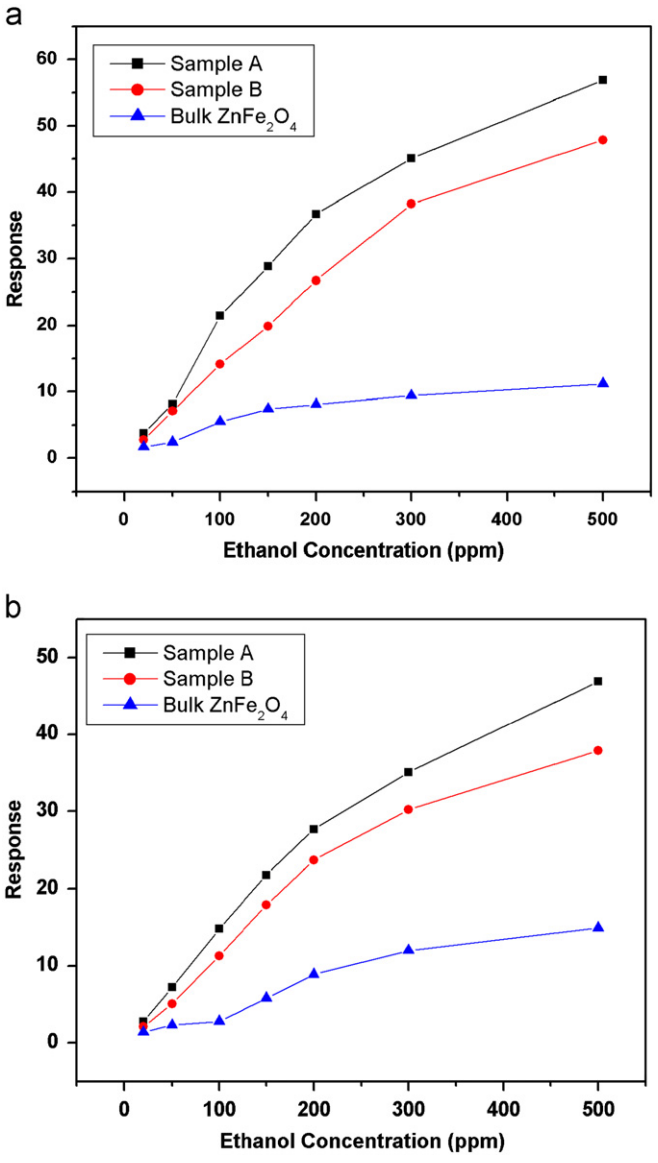

Fig. 4. Relationship between response of sensor and gas concentration of (a) ethanol and (b) hydrogen sulfide.

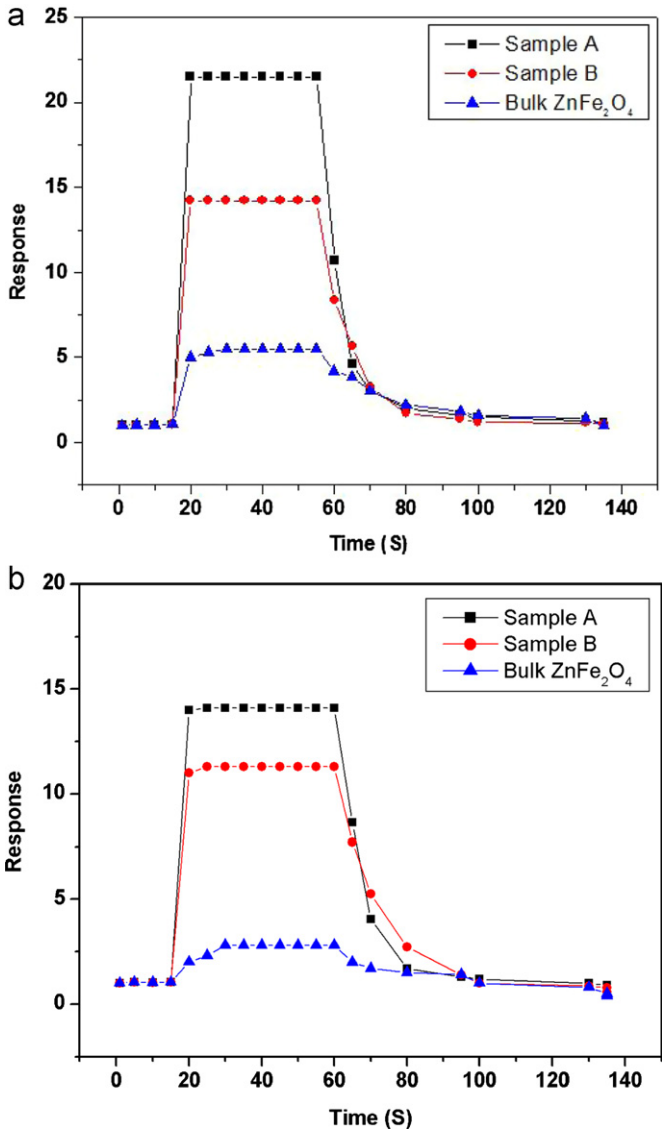

Fig. 5. The response and recovery curves for sensors of (a) ethanol and (b) hydrogen sulfide.

smaller particle size and larger specific surface area. The faster response/recovery characteristics the sensor has, the smaller particles size sample A has. These are accordant with the practical use requirement of gas sensor which should provide not only high response but also rapid response and recovery properties to target gas.

4. Conclusions

In summary, $ZnFe_2O_4$ nanomaterials have been synthesized by solid-phase chemical reaction technique. The method requires only one-step process and the condition of room temperature, which was applied within a few minutes. The gas sensing measurements show that the sensors based on the as-prepared $ZnFe_2O_4$ nanomaterials have not only high response and good selectivity but also rapid response and recovery properties to ethanol and hydrogen sulfide, which is better than bulk materials.

The excellent sensitive properties make as-prepared $ZnFe_2O_4$ nanomaterials ideal candidates for ethanol and hydrogen sulfide gas-sensing devices.

Acknowledgments

This work was financially supported by the Natural Science Foundation of Xinjiang University (Nos. BS100129 and XJEDU2012I03), the Natural Science Foundation of Xinjiang Province (No. 2010211A09), the National Natural Science Foundation of China (Nos. 21101132, 21061013 and 21271151), Xinjiang Autonomous Region with Science and Technology Project Plan (No. 200991101) and Autonomous Regions High Technology Research and Development Program (No. 201016118).

References

[1] Y.N. Xia, P.D. Yang, Y.G. Sun, Y.Y. Wu, B. Mayers, B. Gates, Y.D. Yin, F. Kim, H.Q. Yan, One-dimensional nanostructures: synthesis, characterization, and applications, Advanced Materials 15 (2003) 353–389.

[2] J. Chen, L. Xu, W.Y. Li, X.H. Gou, α-Fe_2O_3 nanotubes in gas sensor and lithium-ion battery applications, Advanced Materials 17 (2005) 582–585.

[3] C.S. Rout, S.H. krishna, S.R.C. Vivekchand, A. Govindaraj, C.N.R. Rao, Hydrogen and ethanol sensors based on ZnO nanorods, nanowires and nanotubes, Chemical Physics Letters 418 (2006) 586–590.

[4] G. Sberveglieri, C. Baratto, E. Comini, G. Faglia, M. Ferroni, A. Ponzoni, A. Vomiero, Synthesis and characterization of semiconducting nanowires for gas sensing, Sensors and Actuators B: Chemical 121 (2007) 208–213.

[5] G. Neri, A. Bonavita, G. Micali, N. Donato, F.A. Deorsola, P. Mossino, I. Amato, B. DeBenedetti, Ethanol sensors based on Pt-doped tin oxide nanopowders synthesised by gel-combustion, Sensors and Actuators B: Chemical 117 (2006) 196–204.

[6] Y.S. Sonawane, K.G. Kanade, B.B. Kale, R.C. Aiyer, Electrical and gas sensing properties of self-aligned copper-doped zinc oxide nanoparticles, Materials Research Bulletin 43 (2008) 2719–2726.

[7] T.S. Zhang, P. Hing, J.C. Zhang, L.B. Kong, Ethanol-sensing characteristics of cadmium ferrite prepared by chemical coprecipitation, Materials Chemistry and Physics 61 (1999) 192–198.

[8] S.W. Tao, F. Gao, X.Q. Liu, O.T. Sørensen, Preparation and gas-sensing properties of $CuFe_2O_4$ at reduced temperature, Materials Science and Engineering B 77 (2000) 172–176.

[9] S.L. Darshane, S.S. Suryavanshi, I.S. Mulla, Nanostructured nickel ferrite: a liquid petroleum gas sensor, Ceramics International 35 (2009) 1793–1797.

[10] X.D. Lou, S.P. Liu, D.Y. Shi, W.F. Chu, Ethanol-sensing characteristics of $CdFe_2O_4$ sensor prepared by sol–gel method, Materials Chemistry and Physics 105 (2007) 67–70.

[11] K. Mukherjee, D.C. Bharti, S.B. Majumder, Solution synthesis and kinetic analyses of the gas sensing characteristics of magnesium ferrite particles, Sensors and Actuators B: Chemical 146 (2010) 91–97.

[12] A.M. Gheidari, E.A. Soleimani, M. Mansorhoseini, S. Mohajerzadeh, N. Madani, W. Shams-Kolahi, Structural properties of indium tin oxide thin films prepared for application in solar cells, Materials Research Bulletin 40 (2005) 1303–1307.

[13] M.R. Mohammadi, D.J. Fray, Semiconductor TiO_2–Ga_2O_3 thin film gas sensors derived from particulate sol–gel route, Acta Materialia 55 (2007) 4455–4466.

[14] X.A. Zhang, W.J. Wu, T. Tian, Y.H. Man, J.F. Wang, Deposition of transparent conductive mesoporous indium tin oxide thin films by a dip coating process, Materials Research Bulletin 43 (2008) 1016–1022.

[15] K. Mukherjee, S.B Majumder, Synthesis process induced improvement on the gas sensing characteristics of nano-crystalline magnesium zinc ferrite particles, Sensors and Actuators B: Chemical 162 (2012) 229–236.

[16] Y.L. Liu, Z.M. Liu, Y. Yang, H.F. Yang, G.L. Shen, R.Q. Yu, Simple synthesis of $MgFe_2O_4$ nanoparticles as gas sensing materials, Sensors and Actuators B: Chemical 107 (2005) 600–604.

[17] P.P. Hankare, S.D. Jadhav, U.B. Sankpal, R.P. Patil, R. Sasikala, I.S. Mulla, Gas sensing properties of magnesium ferrite prepared by co-precipitation method, Journal of Alloys and Compounds 488 (2009) 270–272.

[18] K. Mukherjee, S.B. Majumder, Reducing gas sensing behavior of nano-crystalline magnesium–zinc ferrite powders, Talanta 81 (2010) 1826–1832.

[19] N.Z. Bao, L.M. Shen, W. An, P. Padhan, C.H. Turner, A. Gupta, Formation mechanism and shape control of monodisperse magnetic $CoFe_2O_4$ nanocrystals, Chemistry of Materials 21 (2009) 3458–3468.

[20] S. Tyagi, H.B. Baskey, R.C. Agarwala, V. Agarwala, T.C. Shami, Development of hard/soft ferrite nanocomposite for enhanced microwave absorption, Ceramics International 37 (2011) 2631–2641.

[21] I.H. Gul, A. Maqsood, M. Naeem, M.N. Ashiq, Optical, magnetic and electrical investigation of cobalt ferrite nanoparticles synthesized by co-precipitation route, Journal of Alloys and Compounds 507 (2010) 201–206.

[22] J.E. Tasca, C.E. Quincoces, A. Lavat, A.M. Alvarez, M.G. González, Preparation and characterization of $CuFe_2O_4$ bulk catalysts, Ceramics International 37 (2011) 803–812.

[23] X.F. Chu, D.L. Jiang, Y. Guo, C.M. Zheng, Ethanol gas sensor based on $CoFe_2O_4$ nano-crystallines prepared by hydrothermal method, Sensors and Actuators B: Chemical 120 (2006) 177–181.

[24] S.B. Majumder, K. Mukherjee, Hydrogen sensing characteristics of wet chemical synthesized tailored $Mg_{0.5}Zn_{0.5}Fe_2O_4$ nanostructures, Nanotechnology 21 (2010) 255504–255509.

[25] X.R. Ye, D.Z. Jia, J.Q. Yu, X.Q. Xin, Z.L. Xue, One-step solid-state reaction at ambient temperature-a novel approach to nanocrystal synthesis, Advanced Materials 11 (1999) 941–943.

[26] T.Y. Zhou, X.Q. Xin, Room temperature solid-state reaction-a convenient novel route to nanotubes of zinc sulfide, Nanotechnology 15 (2004) 534–536.

[27] Z.P. Sun, L. Liu, L. Zhang, D.Z. Jia, Rapid synthesis of ZnO nanorods by one-step, room-temperature, solid-state reaction and their gas-sensing properties, Nanotechnology 17 (2006) 2266–2270.

[28] R.Y. Wang, D.Z. Jia, L. Zhang, L. Liu, Z.P. Guo, B.Q. Li, J.X. Wang, Rapid synthesis of amino acid polyoxometalate nanotubes by one-step solid-state chemical reaction at room temperature, Advanced Functional Materials 16 (2006) 687–692.

[29] Y.L. Cao, P.F. Hu, W.Y. Pan, Y.D. Huang, D.Z. Jia, Methanal and xylene sensors based on ZnO nanoparticles and nanorods prepared by room-temperature solid-state chemical reaction, Sensors and Actuators B: Chemical 134 (2008) 462–466.

[30] Y. Zong, Y.L. Cao, D.Z. Jia, P.F. Hu, The enhanced gas sensing behavior of porous nanocrystalline SnO_2 prepared by solid-state chemical reaction, Sensors and Actuators B: Chemical 145 (2010) 84–88.

[31] Z. Jiao, S.Y. Wang, L.F. Bian, J.H. Liu, Stability of SnO_2/Fe_2O_3 multilayer thin film gas sensor, Materials Research Bulletin 35 (2000) 741–745.

[32] K.M. Reddy, L. Satyanarayana, S.V. Manorama, R.D.K. Misra, A comparative study of the gas sensing behavior of nanostructured nickel ferrite synthesized by hydrothermal and reverse micelle techniques, Materials Research Bulletin 39 (2004) 1491–1498.